Desalination and Water Treatment
www.deswater.com

doi: 10.5004/dwt.2017.20550

71 (2017) 182–190
April

Kinetics of divalent mercury reduction by zero-valent iron: the effects of pH, chloride, and dissolved organic carbon

Go-Un Nam[a], Seunghee Han[b], Yongseok Hong[a,*]

[a]*Department of Environmental Engineering, Daegu University, Gyeongsan-si, Gyeongsangbuk-do, Daegu, Korea, Tel. +82-53-850-6694; Fax: +82-53-550-6699; emails: yshong@daegu.ac.kr (Y. Shon), namgwo@gmail.com (G.-U. Nam)*
[b]*School of Environmental Science and Engineering, Gwangju Institute of Science and Technology (GIST), Gwangju, Korea, email: shan@gist.ac.kr*

Received 17 September 2016; Accepted 28 January 2017

ABSTRACT

The effects of pH, Cl^-, and dissolved organic carbon (DOC) on the kinetics of Hg^{2+} reduction to Hg^0 were investigated in anoxic Fe^0–H_2O system. A reaction kinetic model was developed to describe separately the surface-mediated and aqueous phase Hg reduction processes. The Hg^{2+} was rapidly reduced to Hg^0 in the presence of 2 g L^{-1} Fe^0 (0.42 m^2 L^{-1}) within 3 h although the presence of DOC significantly, about an order of magnitude, reduced the reduction kinetics. The zero-valent iron (ZVI) surface area normalized Hg^{2+} reduction rates varied between 0.5 and 2.74 m^{-2} min^{-1}. In the presence of 0.1–10 mg/L DOC, the rates varied between 0.026 and 0.1 m^{-2} min^{-1}. Modeling studies showed that the increase of pH and NaCl concentrations and the decrease of DOC levels increased surface-mediated Hg^{2+} reduction rate. Higher pH seemed to increase the reduction rates and this was attributed to the enhanced adsorption of Hg^{2+} to ZVI surface at higher pH. The Cl^- undergoes strong complexation with Hg^{2+} (i.e., $HgCl^+$, $HgCl_2$, and $HgCl_3^-$) and prevent the adsorption of Hg^{2+} to Fe^0 surface and subsequent reduction. However, the enhanced corrosion and greater release of Fe^{2+} by the pitting corrosion process in the presence of Cl^- affected the overall Hg^{2+} reduction far more significantly, hence, increased Hg^{2+} reduction was observed in the presence of Cl^- in solution. The DOC seemed not only to decrease the reactivity of Hg^{2+} by rendering strong complexation but also to prevent the adsorption of Hg^{2+} to the Fe^0 surfaces thus inhibiting surface reduction.

Keywords: Zero-valent iron; Mercury reduction kinetics; Mercury-contaminated wastewater; Groundwater pollution

1. Introduction

As a contaminant with significant toxicity and environmental persistence, and an ability to contaminate pristine areas via atmospheric transport, mercury (Hg) is often considered to be one of the most dangerous and ubiquitous contaminants in various environmental media [1]. In addition to its occurrence in natural environments, Hg can be easily found in solid wastes and wastewaters produced from various industrial processes [2]. The major sources of Hg in aquatic environments are considered to be atmospheric deposition and surface runoff [3,4]. However, in some locations, Hg in groundwater could be a significant mercury source depending on the hydrological and geochemical settings of a water body [5,6]. Once it is released into the aquatic environment, it transforms to methylmercury, a contaminant which is highly neurotoxic and bioavailable, and poses significant health concerns to aquatic ecosystems and humans. Hence, the removal of Hg from wastewater and groundwater has been extremely important.

Conventional materials used for removing Hg from wastewaters include activated carbon [7], clay minerals [8], zeolites [9], and iron(oxy)hydroxides [10]. To enhance the Hg removal efficacy, thiol-functionalized clay [11], resins [12], mesoporous silica [13], and porous aromatic framework [14] are also synthesized and used as effective sorbents to

* Corresponding author.

remove Hg from wastewaters. Among those various materials for treating mercury from wastewater and contaminated groundwater [15], the use of zero-valent iron (ZVI), a strong, environmentally friendly reducing agent, has drawn great attention as an inexpensive and effective treatment based on previous studies [16,17]. Recently, granular iron powder, elemental copper, and attapulgite clay were chemically treated with elemental sulfur (S), and the effectiveness of the resulting S-impregnated materials as reactive components for groundwater Hg treatment was investigated [18,19].

There are several studies that have investigated Hg removal mechanisms by ZVI. Mercury-contaminated groundwater was treated by ZVI permeable reactive barriers, and mineralogical studies conducted by scanning electron microscopy/energy-dispersive X-ray spectroscopy and X-ray absorption fine structure showed that mercury was precipitated as mercury sulfide in the form of cinnabar and metacinnabar [19]. Artificial Hg-contaminated groundwater was mixed with granular iron fillings being composed of ZVI, and an extended X-ray absorption fine structure (EXAFS) study showed that the major removal mechanisms of Hg was its precipitation onto ZVI corrosion products [18]. A simple study showed that Hg^{2+} was rapidly removed within 2 min in the presence of nano-ZVI (nZVI), and the study proposed that the reduction of Hg^{2+} to Hg^0 was an nZVI surface-mediated phenomenon [17]. The product, Hg^0, was subsequently adsorbed on the nZVI surface.

Although several studies yielded results that prove the effectiveness of ZVI in Hg removal from wastewaters and groundwater, these did not provide detailed insights on Hg removal mechanisms in the presence of environmental factors. For example, Hg^{2+} is strongly complexed with various ligands, such as Cl^-, OH^-, and dissolved organic carbon (DOC) [1], and when Hg^{2+} is complexed with those ligands, the reaction between Hg^{2+} and ZVI could be different. In addition, Cl^- [20] and DOC [21] could affect the performance of ZVI. In the present study, series of laboratory batch experiments were conducted to investigate the kinetics of Hg^{2+} reduction to Hg^0 by commercially available ZVI in anoxic environments. However, Cl^-, DOC, and pH influence on Hg^{2+} reduction rates were examined in the same system. The release of $Fe^{2+}_{(aq)}$ from ZVI and the reduction of Hg^{2+} by $Fe^{2+}_{(aq)}$ were also investigated. The overall results of this work provide insights on Hg^{2+} removal by ZVI.

2. Materials and methods

2.1. Modeling approach

The dominant contaminant removal mechanism of ZVI is known to be a surface-mediated process [22], though ZVI could release Fe^{2+} during its corrosion in water [23]. In such case, Hg^{2+} could be reduced by both in aqueous solution and at the ZVI surface. The reduction of Hg^{2+} by ZVI was considered to occur either on the ZVI surface or in aqueous solution. The reaction kinetic expression at the ZVI surface and in aqueous solution was assumed to be as follows [24–26]:

$$\frac{d[Hg^0]}{dt} = k_s S_A [Hg^{2+}]_{tot} + k_{aq}\left[FeOH^+\right]\left[Hg^{2+}\right]_{tot} \quad (1)$$

where $[Hg^0]$ is the reduced elemental Hg concentration (M), k_s is the surface area normalized lumped first-order reaction rate constant (min^{-1} m^{-2}), S_A is the surface area of ZVI used in this experiments (m^2), $[Hg^{2+}]_{tot}$ is the total Hg^{2+} concentrations in aqueous solution (M), k_{aq} is the aqueous phase Hg reduction second order reaction rate constant (M^{-1} min^{-1}), and $[FeOH^+]$ is the aqueous phase $FeOH^+$ concentrations at a given pH.

In aqueous solution, it is assumed that Hg^{2+} is reduced to Hg^0 by an overall second-order kinetic expression with respect to $FeOH^+$ and total Hg^{2+} in aqueous solution. A previous study [26] showed that $FeOH^+$ has higher activity compared with other Fe^{2+} species, such as free Fe^{2+} and $Fe(OH)_2$, despite its presence at significantly lower concentrations than other species, due to its higher metal basicity and lower reduction potential ($FeOH^{2+}$/$FeOH^+$, E^0 = 0.34 V_{SHE}; Fe^{3+}/Fe^{2+}, E^0 = 0.77 V_{SHE}). The concentrations of $FeOH^+$ at a certain pH are calculated using the stability reactions and constants summarized in Table 1.

In Eq. (1), the k_{aq} was first evaluated using experimental data obtained in experiments conducted in the presence of 1 mM $Fe^{2+}_{(aq)}$ without ZVI. Then, the Hg^{2+} reduction experiments by ZVI were conducted and k_s was evaluated by employing Runge–Kutta order 4 and Visual Basic complier in Microsoft Excel® at a fixed k_{aq}. The k_s was determined to minimize the sum of squared errors between experimental data and modeling results. The standard deviation (68% confidence interval) was evaluated using statistical methods [27]. In addition to the kinetic modeling, WHAM7 (version 7.0.5) was used to investigate the equilibrium partitioning of metals to DOC [28].

2.2. Hg^{2+} reduction experiments

All solutions were prepared using deionized water with resistivity of 18 MΩ cm^{-1} and American chemical society reagent grade or higher grade chemicals purchased from Acros Chemical (New Jersey, USA), Fisher Chemical (Massachusetts, USA), and Sigma Aldrich (Missouri, USA). All glassware and plasticware were serially soaked in detergent and 50% concentrated HCl for >1 d, rinsed with deionized water several times, and dried in a clean bench equipped with an high efficiency particulate absorber filter.

Table 1
The complexation reactions of Fe^{2+} and Hg^{2+} in aqueous phase and their stability constants [26]

#	Reactions	log*K*
1	$Fe^{2+} + H_2O = FeOH^+ + H^+$	–9.4
2	$Fe^{2+} + 2H_2O = Fe(OH)_2 + 2H^+$	–20.49
3	$Fe^{2+} + 3H_2O = Fe(OH)_3^- + 3H^+$	–28.99
4	$Hg(OH)_2 + 2H^+ = Hg^{2+} + 2H_2O$	6.19
5	$Hg(OH)_2 + H^+ = HgOH^+ + 2H_2O$	2.8
6	$Hg(OH)_2 + H_2O = Hg(OH)_3^- + H^+$	–14.9
7	$Hg(OH)_2 + 2H^+ + Cl^- = HgCl^+ + 2H_2O$	13.49
8	$Hg(OH)_2 + 2H^+ + 2Cl^- = HgCl_2 + 2H_2O$	20.19
9	$Hg(OH)_2 + 2H^+ + 3Cl^- = HgCl_3^- + 2H_2O$	21.19
10	$Hg(OH)_2 + 2H^+ + 4Cl^- = HgCl_4^{2-} + 2H_2O$	21.80
11	$Hg(OH)_2 + H^+ + Cl^- = HgClOH + H_2O$	10.44

All Hg^{2+} reduction experiments were conducted in 40 mL amber serum bottles at 20°C (±3). The bottles were capped with 3-mm thick butyl rubber stopper, which has air in and out ports made of 1 mm diameter Teflon tubing. The bottles were filled with 20 mL of deionized water buffered at pH 7.0 (±0.2) with 10 mM 4-(2-hydroxyethyl)-1-piperazineethanesulfonic acid (HEPEs). The 20 mL solution in 40 mL amber bottle was purged with 99.9999% N_2 gas for 4 h with a flow rate of 50 mL/min to remove O_2 from the solution. While constantly purging the solution, 20 μL of 10 μM $HgCl_2$ stock solution (10 nM Hg^{2+}) was added to the reactor. The Hg^{2+} reduction experiments were initiated by adding 0.04 g of ZVI (Acros (New Jersey, USA), 70 mesh, ~212 μm diameter, 0.21 m^2 g^{-1}).

To collect reduced Hg^0, the purged out gas was passed through 10 mL of 0.6% $KMnO_4$ and 5% H_2SO_4 in 15 mL polypropylene tubing [29]. A preliminary experiment showed that the $KMnO_4$ solution was effective in capturing Hg^0 in gas stream. The $KMnO_4$ solution was replaced at 20, 40, 60, 90, 120, and 180 min and total Hg in the $KMnO_4$ was analyzed using BrooksRand Model III cold vapor atomic fluorescence detector and United States environmental protection agency method 1631.To measure the Hg^0 adsorbed on to the ZVI surface, the solution pH was lowered to 1.5 by adding 125 μL concentrated HNO_3 and purged with N_2 gas for 60 min and evaporated Hg^0 was trapped in 10 mL of $KMnO_4$ solution. Then, 0.8 mL of water sample was taken after magnetic ZVI separation using neodymium magnets (~3,000 Gs).

The effects of pH, DOC, and Cl^- on Hg^{2+} reduction to Hg^0 by ZVI were investigated. To investigate the pH effect, pH 6.0 (±0.2) 2-(N-morpholino)ethanesulfonic acid (MES) buffer and pH 8.0 (±0.2) HEPEs buffer were used and both DOC and Cl^- concentrations were fixed at zero during the experiment. While fixing pH and NaCl concentrations at 7.0 and zero, respectively, DOC concentrations were varied from 0.1 to 10 mg C/L by adding 1,000 mg C/L Suwanne River natural organic matter (International Humic Substances Society) to explore DOC effects. The effects of NaCl on Hg^{2+} reduction were examined by varying NaCl concentrations from 0.001 to 0.1 M properly adding 1 M NaCl, and pH and DOC concentrations were 7.0 and zero, respectively, during the experiment. When DOC and NaCl effects were investigated, the orders of experiments were slightly modified. To fully complex Hg^{2+} with DOC and Cl^-, Hg^{2+} and DOC or Cl^- were added to the 20 mL buffered solution at the same time. The solution was equilibrated for 4 h while constantly being purged with N_2. The Hg^{2+} adsorption on humic acids occurs rapidly within 3 h, according to the literature [30,31].

Since $Fe^{2+}{}_{(aq)}$ is released from ZVI in Fe^0–H_2O system and the $Fe^{2+}{}_{(aq)}$ could reduce Hg^{2+} in aqueous solution [26], separate experiments were conducted using experimental setup identical to Hg^{2+} reduction experiments. After adding 0.04 g ZVI to 20 mL solution, the 10–20 μL water samples were taken at 30, 60, 90, 120, and 180 min and aqueous phase Fe^{2+} was measured by spectrophotometric method using FerroZine [32]. To prevent oxygen intrusion to the solution, the samples were taken rapidly within a few seconds. A magnet was placed at the bottom of the 40 mL amber bottles whenever samples were taken to prevent iron particle interference.

The reduction of Hg^{2+} by $Fe^{2+}{}_{(aq)}$ was also investigated to support the experimental results obtained from Hg^{2+} reduction by ZVI. Similar experimental approaches with Hg^{2+} reduction by ZVI were employed, although 0.4 mL of 0.05 M Fe^{2+} ($FeSO_4$ dissolved in 0.1 M HNO_3) was added to the batch bubbling system instead of ZVI to obtain the final Fe^{2+} concentration of 1 mM. The pH, Cl^-, and DOC levels were changed from 6 to 8, 0.001 to 0.1 M, and 0.1 to 10 mg/L, respectively.

3. Results and discussion

3.1. Release of Fe^{2+} from ZVI

Past studies have well established that the corrosion on the ZVI surface proceeds, $Fe^{2+}{}_{(aq)}$ is released, which subsequently reduces Hg^{2+} in the solution. Under such $Fe^{2+}{}_{(aq)}$ releasing condition, Hg could be reduced by both ZVI and $Fe^{2+}{}_{(aq)}$ depending on solution chemistry. The release of total $Fe^{2+}{}_{(aq)}$ from ZVI in three different pH values and varying Cl^- and DOC concentrations is shown in Fig. 1 and $FeOH^+$ concentration, which is reactive to Hg^{2+} reduction, are shown in Fig. 2. The dissolution of $Fe^{2+}{}_{(aq)}$ by the ZVI corrosion was simply described by the following sigmoid curve fitting:

$$[Fe^{2+}]_{tot} = \frac{a}{1+\exp\left(-\left(t-x_0\right)/b\right)} \quad (2)$$

where $[Fe^{2+}]_{tot}$ is the measured total Fe^{2+} concentrations in solution (M), a, b, and x_0 are the fitting parameters, and t is time (min). The fitting parameters are shown in Table 2.

Generally, the release of $Fe^{2+}{}_{(aq)}$ from ZVI follows an S-shape curve (Fig. 1). There was initial lag period for the first 60 min, which was followed by a gradual increase of $[Fe^{2+}{}_{(aq)}]$. At time 180 min, the highest Fe^{2+} concentrations was around 2.5 mM when the pH is 6, although almost no Fe^{2+} was detected in pH 8 solution. At pH 7, the dissolved NaCl seemed to accelerate the Fe^0 corrosion and increase the release of Fe^{2+}. In the absence of NaCl in the solution, the Fe^{2+} concentrations were around 0.5 mM; however, the 0.001–0.1 M NaCl increased the Fe^{2+} concentrations up to 1.2 mM. This is considered to be due to the enhanced ZVI corrosion in the presence of Cl^- by the pitting corrosion mechanism. The irregularly localized dissolution on the ZVI surface creates a net positive charge, which attracts the negatively charged Cl^- ions thus forming metal chlorides via neutralization reaction [20]. Hydrolysis of these chloride salts forms a metal hydroxide and hydrochloric acid and creates pits, which serve as a continuous source of Fe^{2+} and electrons.

Unlike Cl^-, the presence of DOC did not affect the release of Fe^{2+} significantly. Windermere humic aqueous model (WHAM) speciation model shown in Fig. 3(a) suggested that around neutral pH (6–8), 99% of aqueous phase Fe^{2+} did not make complexes with DOC when Fe^{2+} concentration is 1 mM and DOC concentration is 10 mg/L. Hence, the Fe^{2+} solubility would not be increased by DOC. It is possible that DOC may block reactive surface areas of Fe^0 [33] and prevent the release of Fe^{2+} into solution. However, these behaviors were not observed during 180 min of our experimental time due to slower adsorption of DOC to iron [34].

3.2. Reduction of Hg^{2+} by $Fe^{2+}{}_{(aq)}$

The Hg^{2+} reduction to Hg^0 by 1 mM Fe^{2+} in various pH, and Cl^- and DOC concentrations are shown in Fig. 4. The reduction kinetic parameters, k_{aq} (M^{-1} min^{-1}), introduced in

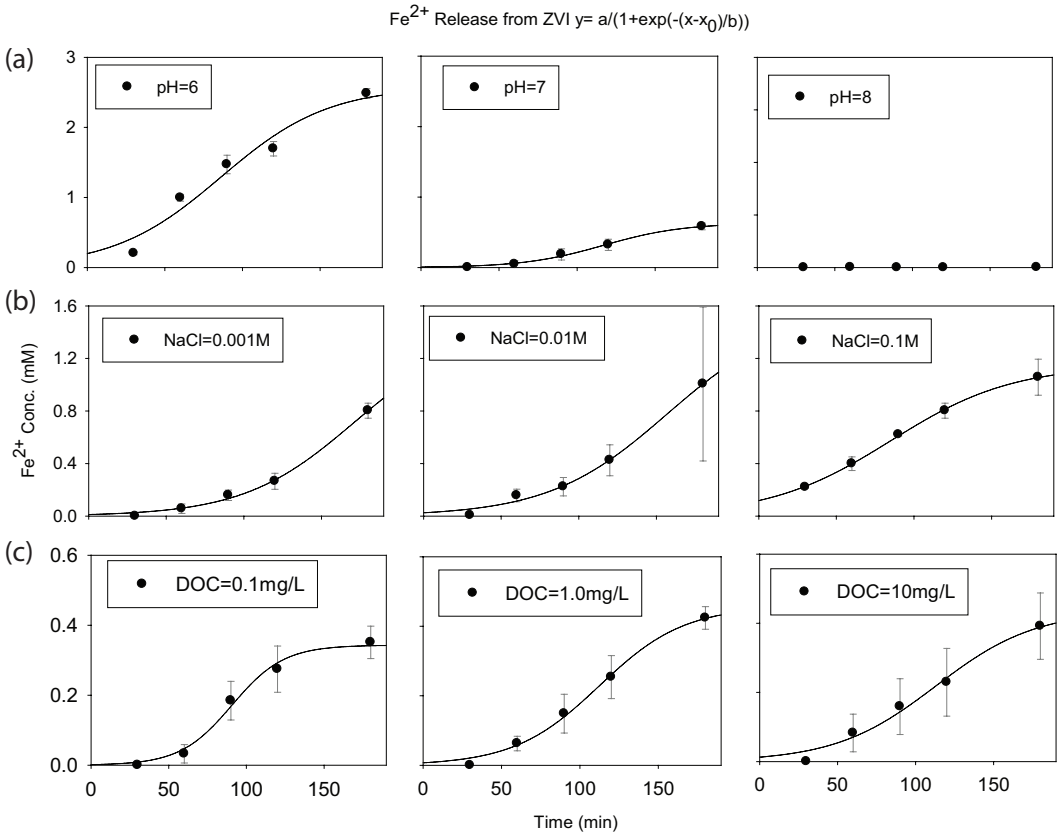

Fig. 1. Effects of: (a) pH, (b) NaCl, and (c) pH on the dissolution of total $Fe^{2+}_{(aq)}$ from ZVI. Sigmoid curve ("S" shape, $y = a/(1+\exp(-(x-x_0)/b))$) fitting was used to empirically model the release of $Fe^{2+}_{(aq)}$ from ZVI. The initial concentration of Hg^{2+} was 10 nM and pH of (b) and (c) was 7.0. Error bars represent standard deviation of triplicate data. DOC source was Suwannee River natural organic matter (NOM).

Eq. (2), were evaluated from each figure using Sigma Plot® and are shown in Table 3. The $FeOH^+$ concentrations were assumed to be constant during the experiments since the oxidized $Fe^{2+}_{(aq)}$ concentration would be extremely low due to the low Hg^{2+} concentration (10 nM). The calculated $FeOH^+$ concentrations were 3.98×10^{-4}, 3.98×10^{-3}, and 3.83×10^{-2} mM when pH was 6.0, 7.0, and 8.0, respectively, which were 2–3 orders of magnitude lower than the added total Fe^{2+}.

Generally, when the pH increased, the Hg^{2+} reduction kinetics became faster, while the presence of NaCl and DOC decreased the Hg^{2+} reduction rates by Fe^{2+} in aqueous solution (Fig. 4). Under the given experimental conditions, the pH seemed to have a drastic effect on Hg^{2+} reduction: when pH is 6, <10% of Hg^{2+} was reduced whereas 99% of Hg^{2+} was reduced when pH is 8.2, during 180 min experimental period. The second-order kinetic reaction rate constants (k_{aq}) varied under the different experimental conditions, but were confined within an order of magnitude between 0.94×10^3 and 6.9×10^3 M^{-1} min^{-1} (Table 3). In the absence of Cl^- and DOC, when the pH are 6, 7, and 8, the k_{aq} were 5.57 (±9.55), 6.90 (±0.48), and 2.43 (±0.45) M^{-1} min^{-1}, respectively.

The k_{aq} was slightly decreased to 2.52–4.11 M^{-1} min^{-1}, in the presence of Cl^- and significantly decreased to 0.97–2.71 M^{-1} min^{-1} in DOC containing solutions (Table 3). There can be several reasons for the decrease of Hg^{2+} reduction kinetics by Cl^-, but one of the reasons could be production of calomel (Hg_2Cl_2) during the reactions. The reduction of Hg^{2+} by Fe^{2+} is a two-step process. Initially, Hg^{2+} is reduced to Hg^+ by one electron donated from $FeOH^+$, which is the thermodynamically favorable pathway over direct reduction to Hg^0 because E^0 for the Hg^{2+}/Hg_2^{2+} couple (0.914 V_{SHE}) is greater than that for the Hg^{2+}/Hg^0 couple (0.85 V_{SHE}). Then, Hg^+ can be further reduced to Hg^0 by another electron donated from another $FeOH^+$ molecule. However, in the presence of Cl^-, the Hg^+ can form calomel (Hg_2Cl_2), and the reduction potential of calomel to Hg^0 ($Hg_2Cl_2 + 2e^- \rightarrow 2Hg^0 + 2Cl^-$, $E^0 = 0.27$ V_{SHE}) is lower than that of Hg^+ ($Hg^+ + e^- \rightarrow Hg^0$, $E^0 = 0.80$ V_{SHE}), hence may then result in slower reduction to Hg^0 [35]. The presence of DOC could trigger a competition between DOC and other groundwater and wastewater pollutants such as As(III) and As(V) [36]. It is also assumed that the adsorption of DOC, in the form of humic acid, inhibits the corrosion of Fe, which in turn prolongs the lifetime of ZVI [33] reducing [$Fe^{2+}_{(aq)}$], which is consistent with our observations shown in Fig. 1.

The k_{aq} measured at the pH 6 and 7 were comparable with a value, 7.19×10^3 M^{-1} min^{-1}, suggested from the previous study [26]. In the previous study, the following equation was used to evaluate the second-order reaction rate constants:

$$\frac{d[Hg^0]}{dt} = k_{aq}\left[FeOH^+\right]\left[Hg(OH)_2\right] \quad (3)$$

Assuming $Hg(OH)_2$ is the most reactive Hg species compared with other Hg species, such as Hg^{2+}, $Hg(OH)^+$, etc. In the present study, the total Hg^{2+} concentrations were used to study reduction kinetics, instead of $Hg(OH)_2$. The WHAM generated

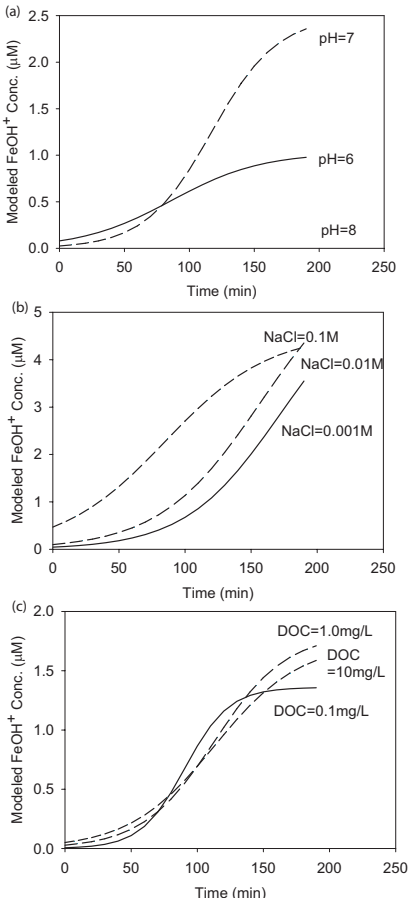

Fig. 2. Calculated $FeOH^+$ concentrations during the release of total $Fe^{2+}_{(aq)}$ from ZVI, which is shown in Fig. 1.

Fig. 3(b) shows that in the absence of Cl^- and DOC, and in pH ranges between 6 and 8, >99% of Hg^{2+} species was present as $Hg(OH)_2$. Hence, the current study's k_{aq} values evaluated at three different pH levels are comparable with the previous study [26].

While the k_{aq} measured at pH 6 and 7 were close to those reported value (7.19×10^3 M^{-1} min^{-1}), and k_{aq} at pH 8 were lower, which is probably caused by experimental artifacts such as rapid reduction of Hg^{2+} at high pH. If $Hg(OH)_2$ concentrations were used to predict Hg^{2+} reduction to Hg^0 in the presence of Cl^- and DOC, the k_{aq} values become significantly larger than the data shown in Table 3. For example, the calculated $Hg(OH)_2$ concentrations in the presence of 0.01 M Cl^- and 1.0 mg/L DOC at pH 7 is only 3.7×10^{-3} and 2×10^{-9} nM, respectively, as shown in Figs. 3(c) and (d). To fit the observed Hg^{2+} reduction, k_{aq} values should be increased by 3 and 9 orders of magnitude, which are not comparable with the reported data. Probably, $Hg(OH)_2$ is not the only species that reacts with $Fe(OH)^+$, but Hg–Cl complexes ($HgCl^+$, $HgCl_2$, and $HgCl_3^-$) and Hg–DOC complex are also reactive and can be reduced by $Fe(OH)^+$.

3.3. Reduction of Hg^{2+} by $Fe^0_{(s)}$

The reduction of Hg^{2+} to Hg^0 by ZVI at various near neutral pH and the effects of Cl^- and DOC on the Hg^{2+} reduction

Table 2
Sigmoid curve ("S" shape y = a / (1 + exp(– (x – x_0) / b))) fitting parameters for describing the release of $Fe^{2+}_{(aq)}$ from ZVI

Solution chemistry	*a*	*B*	x_0	R^2
pH = 6.0 (10 mM MES)	2.58	34.7	86.2	0.96
pH = 7.0 (10 mM HEPEs)	0.629	25.5	117	0.99
pH = 8.0 (10 mM HEPEs)[a]	NA[b]	NA	NA	NA
pH = 7.0 + 10^{-3} M NaCl	1.42	35.6	171	1.0
pH = 7.0 + 10^{-2} M NaCl	1.56	38.2	157	0.99
pH = 7.0 + 10^{-1} M NaCl	1.15	39.3	85.1	1.0
pH = 7.0 + 0.1 mg/L DOC	0.343	16.7	90.7	0.99
pH = 7.0 + 1.0 mg/L DOC	0.457	27.2	113	1.0
pH = 7.0 + 10 mg/L DOC	0.437	32.2	113	0.98

Note: Experimental results are shown in Fig. 1.
[a]Sigmoid curve was not evaluates since no Fe^{2+} was released in the experimental condition.
[b]NA — not available.

are summarized in Fig. 5 and modeled results are shown in Fig. 6. The ZVI surface-mediated Hg^{2+} reduction kinetic rate constants were evaluated by introducing the known k_{aq} and the Fe^{2+} release kinetic in Eqs. (2) to (1). Then, the k_s in Eq. (1) becomes the only fitting parameter and is changed to minimize the sum of squared errors between modeling data and the overall Hg^{2+} reduction data. The best fitted k_s and standard deviation (68% confidence interval) are listed in the third column of Table 3. The mass balance calculation of Hg, i.e., total purged Hg (Hg^0 trapped in $KMnO_4$ solution) for 180 min, 1-h purged Hg after decreasing the solution pH to 1.5 (Hg^0 potentially adsorbed to ZVI surface), and remaining Hg in the solution (not reduced Hg^{2+}) are shown in Fig. 7.

Generally, the overall Hg^{2+} reduction (combined reduction in solution and on the ZVI surface) showed some initial lag period for the first 5–10 min followed by a rapid reduction of Hg^{2+} for 180 min. The modeling results showed that >70% of Hg^0 was reduced by the ZVI surface in the absence of Cl^- and DOC. When pH is 6.0, ZVI surface reduced 70% of evaporated Hg^0, and the remaining 30% was expected to be reduced in solution by Fe^{2+} released from the corrosion of ZVI. When pH is 7.0, ZVI surface reduced 83% of total evaporated Hg^0, and at pH 8.0, no aqueous phase Fe^{2+} was observed, hence, the 100% of the released Hg^0 was considered to be reduced on the ZVI surface. This observation suggested that when the pH is increasing, the ZVI surface-mediated Hg^{2+} reduction is also increasing.

When NaCl concentrations are 0.001, 0.01, and 0.1 M, the Hg^{2+} reduced at the ZVI surface were 80%, 86%, and 89%, respectively, suggesting that more Hg^{2+} was reduced at the surface by the increase of NaCl concentrations. The DOC seemed to significantly retard the Hg^{2+} reduction both in aqueous solution and at surface. Only 17%, 35%, and 40 % of Hg^{2+} were evaporated as Hg^0 in the presence of 10, 1.0 and 0.1 mg/L DOC, respectively, during the experimental time span, which suggested that the increase of DOC decreased the overall Hg^{2+} reduction by ZVI. In addition, among the released Hg^0, only 25%–42% of the evaporated Hg^0 was reduced by ZVI

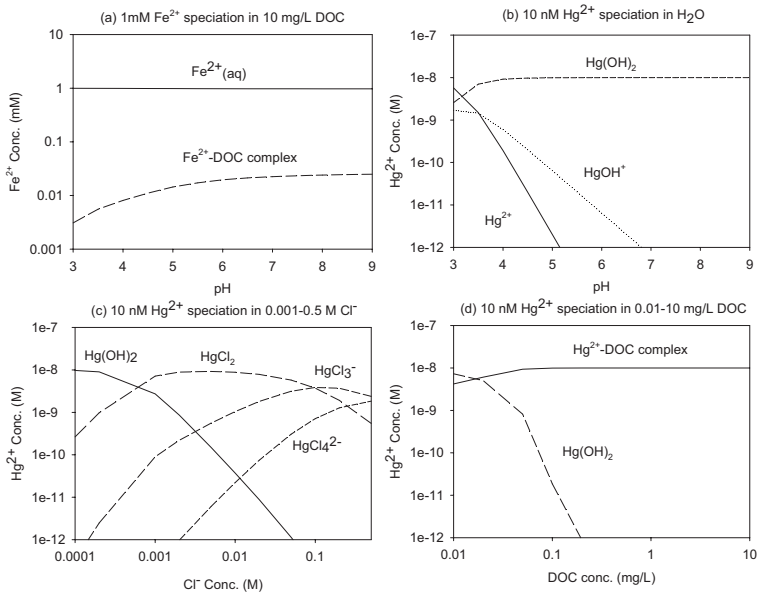

Fig. 3. WHAM 7 modeled Hg speciation at 20°C: (a) aqueous phase 1 mM Fe^{2+} speciation in the presence of 10 mg/L DOC (modeled as humic acid), (b) aqueous phase 10 nM Hg^{2+} speciation in pure water, (c) aqueous phase 10 nM Hg^{2+} speciation as a function of Cl^- concentrations, and (d) aqueous phase 10 nM Hg^{2+} speciation in the presence of 0.01–10 mg/L DOC (humic acid) [28].

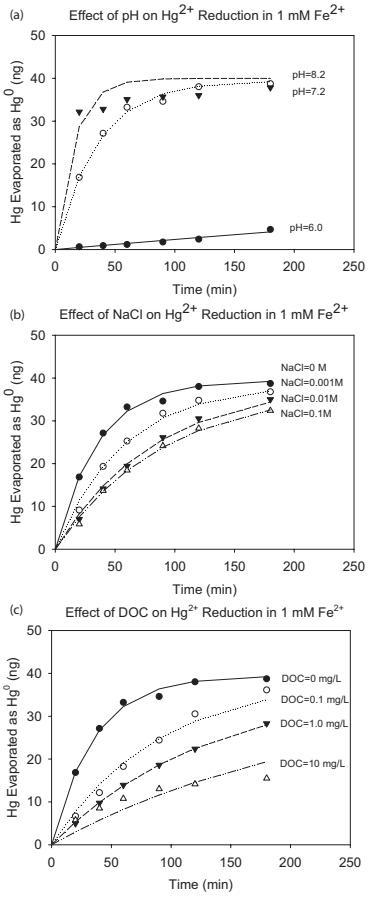

Fig. 4. Effects of: (a) pH, (b) NaCl, and (c) DOC on the Hg^{2+} reduction and evolution of Hg^0 by $Fe^{2+}_{(aq)}$. The initial concentration of Hg^{2+} was 10 nM and pH of (b) and (c) was 7.0 (±0.2). Suwannee River NOM was used as a DOC source.

Table 3
Pseudo-second-order Hg^{2+} reduction kinetic rate constants, k_{aq} (10^3 M^{-1} min^{-1}) and the ZVI surface-mediated reduction kinetic rate constants, k_s (m^{-2} min^{-1})

Solution chemistry	k_{aq} (10^3 M^{-1} min^{-1})	k_s (m^{-2} min^{-1})
pH = 6.0 (10 mM MES)	5.57 (±9.55)	0.49 (±0.19)
pH = 7.0 (10 mM HEPEs)	6.90 (±0.48)	1.10 (±0.43)
pH = 8.0 (10 mM HEPEs)	2.43 (±0.45)	0.90 (±0.11)
pH = 7.0 + 10^{-3} M NaCl	4.11 (±0.35)	0.96 (±0.37)
pH = 7.0 + 10^{-2} M NaCl	2.87 (±0.20)	1.43 (±0.43)
pH = 7.0 + 10^{-1} M NaCl	2.52 (±0.25)	2.74 (±0.68)
pH = 7.0 + 0.1 mg/L DOC	2.71 (±0.45)	0.098 (±0.025)
pH = 7.0 + 1.0 mg/L DOC	1.74 (±0.76)	0.098 (±0.043)
pH = 7.0 + 10 mg/L DOC	0.94 (±1.3)	0.026 (±0.023)

Note: The experimental conditions to evaluate k_{aq} were 1 mM Fe^{2+} in 20 mL buffered solution spiked with 40.4 ng (=10 nM) $HgCl_2$. The k_s was evaluated with 0.04 g ZVI (0.21 m^2 g^{-1}) in 20 mL solution spiked with 40.4 ng (=10 nM) $HgCl_2$. The calculated ZVI surface area in the solution is 0.42 m^2 L^{-1}.

surface, which is significantly lower compared with other experimental conditions in the present study. These observations suggest that when the pH is decreasing, and NaCl and DOC concentrations area increasing, which are the cases of increasing aqueous phase Hg^{2+} solubility due to the formation of non-adsorbing mercury complexes [28,29], subsequently decreasing the adsorption of Hg^{2+} to the ZVI surfaces and affecting the Hg^{2+} reduction by ZVI.

The changes of ZVI surface activities by the changes of solution chemistry are inferred from the fitted k_s shown

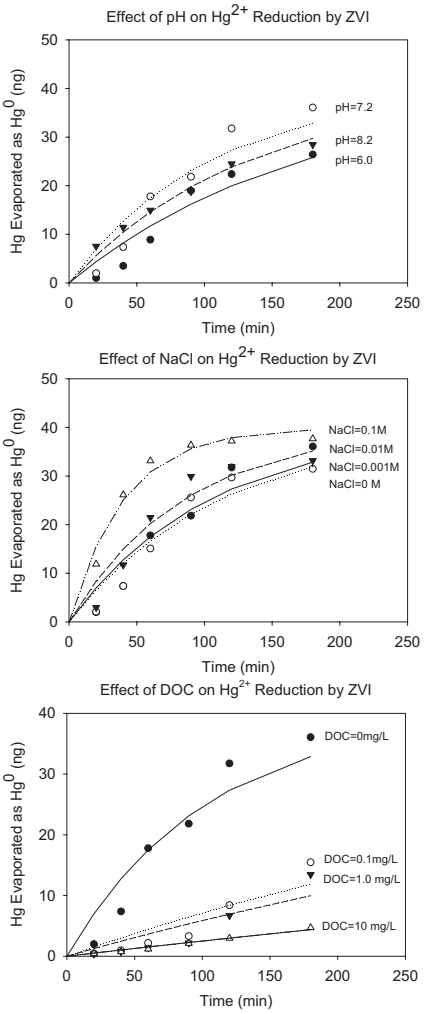

Fig. 5. Hg^{2+} reduction and evolution of Hg^0 by ZVI.

in Table 3. The ZVI surface-mediated Hg^{2+} reaction rate constants, k_s, were 0.49 (±0.19), 1.1 (±0.43), and 0.90 (±0.11) m^{-2} min^{-1} when the pH were 6.0, 7.0, and 8.0, respectively. The rate constants were relatively constant in the given near neutral pH conditions.

The k_s in the presence of Cl^- concentrations were generally higher than in the absence of Cl^-, and the increase was more significant when the Cl^- concentration was higher. The k_s was 2.74 (±0.68) m^{-2} min^{-1} when the Cl^- concentration was 0.1 M, and the value was almost three times higher than 1.10 (±0.43) m^{-2} min^{-1} that was found when the Cl^- concentration was 0 M. The increase of ZVI surface activities by the increase of NaCl was the opposite to the trend observed in solution, where k_{aq} was decreased by the increase of Cl^- concentrations, which is known as a corrosion promoter [20].

The presence of DOC showed a more contrasting effect on ZVI surface-mediated Hg^{2+} reduction since the increase of DOC concentration significantly reduced the k_s. When DOC concentrations were 0.1, 1.0, and 10 mg/L, the k_s were 0.098 (±0.025), 0.098, (±0.043), and 0.026 (±0.023) m^{-2} min^{-1}, respectively, which were more than an order of magnitude lower than the k_s without DOC. These observations provide that when the pH and NaCl concentrations are increasing, the ZVI surface activities are increased, probably by the enhanced corrosion of ZVI surface. In case of NaCl effect, the postulation is consistent with the pitting corrosion processes previously described. On the other hand, when DOC concentrations are increasing, the ZVI surface activities are decreased, probably by the blocking of active ZVI surface by DOC.

As shown above, the overall Hg^{2+} reduction kinetics to Hg^0 by ZVI can be affected by the complex interactions between Hg^{2+} and ZVI as well as the corrosion of ZVI, which are complicated by solution chemistry. The increase of pH would generally increase the Hg^{2+} reduction since the environment is more favorable for Hg^{2+} to adsorb to the ZVI surface, and the higher pH (only in between 6 and 8) seemed to corrode ZVI more and enhance the surface activities. In case of NaCl, higher NaCl would decrease the Hg^{2+} sorption to ZVI surface, however, increase the corrosion of ZVI and surface activities, hence, NaCl was favorable to Hg^{2+} reduction. This behavior was in contrast to the Cl^- effects on Hg^{2+} reduction by magnetite [29]. The study argued that the Cl^- complexed with Hg^{2+} in aqueous phase and prevented the adsorption of Hg^{2+} to the magnetite surface, hence, the overall Hg^{2+} reduction rates were decreased by the increase of Cl^- concentrations. Probably, the structural Fe^{2+} in the magnetite was resistant to corrosion in the presence of Cl^- in the acidic (pH between 4.8 and 6.7) condition. DOC generally decreased Hg^{2+} not only by preventing Hg^{2+} attachment to the surface, but also probably by blocking available ZVI surface.

3.4. Implications

There are several studies that used ZVI to remove Hg in groundwater and wastewater [18,19]. Usually, Hg-contaminated groundwater could be enriched with DOC [5] and Hg containing wastewaters, for example, flue gas desulfurization system, can have extremely high levels of Cl^- [37]. In such cases, designing ZVI-based Hg treatment technologies should consider the effects of those organic and inorganic ligands on Hg^{2+} removal. The Cl^- enhances surface activities by improving corrosions and the DOC significantly reduces the reaction rates of ZVI, hence, appropriate rates should be used. Also, the removal rates are generally evaluated in dilute ZVI concentrations, and in this case, the rates can be the mixed rates in solution and on surface. Especially, rates evaluated for Hg reduction could have been overestimated by aqueous phase reduction, and the direct application of the mixed rate to higher density ZVI treatment technologies, such as packed bed, could bias the removal or reduction results. Careful evaluation of ZVI removal rates in dilute solution is necessary for pollutants like Hg. Lastly, present study can be expanded to develop wastewater treatment processes that employ Hg^{2+} reduction by ZVI, followed by purging the Hg^0 to gas phase, which is subsequently adsorbed on sorption tower. This type of processes will selectively remove Hg^{2+} from waters and can be applied to the Hg recovery from wastewaters.

4. Conclusions

The effects of environmental factors on the kinetics of Hg^{2+} reduction to Hg^0 were investigated in anoxic Fe^0–H_2O system

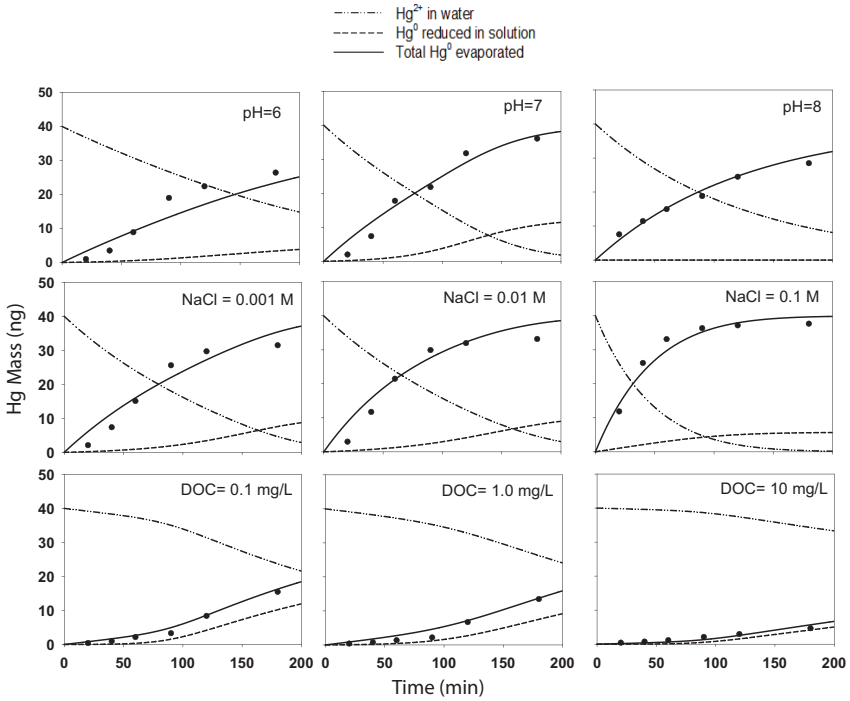

Fig. 6. The modeling of Hg^{2+} reduction kinetics by ZVI using Eq. (1). The kinetic rates, k_{aq} and k_s, are shown in Table 3. Data points indicate experimental results. Initial Hg^{2+} concentration was 10 nM, and pH of DOC and NaCl test was 7.0 (±0.2). Suwannee River NOM was used as a DOC source.

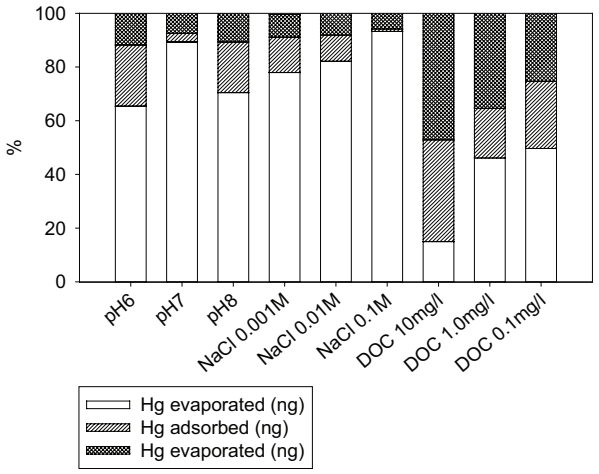

Fig. 7. Mass balance results of Hg^{2+} reduction by ZVI. The evaporated Hg was the total and cumulative purgeable Hg trapped in $KMnO_4$ solution (0–180 min), the Hg adsorbed is the 1-h purged Hg after decreasing the solution pH to around 1.5 (180–240 min), and the Hg in water is the Hg remaining in solution (at 240 min).

using a set of ordinary differential and algebraic equations to separate the surface-mediated and aqueous phase Hg reduction processes. The Hg^{2+} was rapidly reduced to Hg^0 in the presence of 2 g/L Fe^0 within 3 h, and modeling studies showed that Hg^{2+} reduction at the surface of ZVI is heavily dependent on solution chemistry. The ZVI surface-mediated Hg reduction rates were tripled when NaCl concentration was increased from 0.001 to 0.1 M even though the formation of calomel (Hg_2Cl_2) is suspected to inhibit the reduction process in aqueous phase. The Hg^{2+}–DOC interaction decreased the Hg^{2+} reduction rates significantly, by an order of magnitude. The decreased reactivity of Hg^{2+} may be a result of strong complexation with DOC that prevents sorption of Hg^{2+} to the Fe^0 surfaces thus inhibits surface reduction. The model obtained by fitting the empirically obtained data could help predicting the reduction of mercury in wastewater and groundwater and provide solid information on the design of various Hg removal technologies.

Acknowledgments

This research was supported by Basic Science Research Program through the National Research Foundation of Korea (NRF) funded by the Ministry of Science, ICT and Future Planning (grant number: 2015R1C1A1A02037559) and by the Korea Ministry of Environment GAIA project (2016000550002). Authors thank Donghak Lee and Kurt Louis Solis for assisting Hg analysis and correcting grammatical errors in manuscript.

References

[1] W.F. Fitzgerald, C.H. Lamborg, Geochemistry of Mercury in the Environment, E.D. Holland, K.K. Turekian, Eds., Treatise on Geochemistry, Elsevier–Pergamon, Oxford, 2004, pp. 107–148.
[2] UNEP, Global Mercury Assessment 2013: Sources, Emissions, Releases and Environmental Transport, UNEP Chemicals Branch, Geneva, Switzerland, 2013.
[3] C.D. Knightes, Development and test application of a screening-level mercury fate model and tool for evaluating wildlife exposure risk for surface waters with mercury-contaminated sediments (SERAFM), Environ. Modell. Software, 23 (2008) 495–510.

[4] R.B. Ambrose Jr., I.X. Tsiros, T.A. Wool, Modeling mercury fluxes and concentrations in a Georgia watershed receiving atmospheric deposition load from direct and indirect sources, J. Air Waste Manage. Assoc., 55 (2005) 547–558.
[5] C.H. Lamborg, D.B. Kent, G.J. Swarr, K.M. Gretchen. T. Kading, A.E. O'Connor, G.M. Fairchild, D.R. LeBlanc, H.A. Wiatrowski, Mercury speciation and mobilization in a wastewater-contaminated groundwater plume, Environ. Sci. Technol., 47 (2013) 13239–13249.
[6] J. Jeong, G. Kim, S. Han, Influence of trace element fluxes from submarine groundwater discharge (SGD) on their inventories in coastal waters off volcanic island, Jeju, Korea, Appl. Geochem., 27 (2012) 37–43.
[7] C.P. Huang, D.W. Blankenship, The removal of mercury(II) from dilute aqueous solution by activated carbon, Water Res., 18 (1984) 37–46.
[8] H. Farrah, W. Pickering, The sorption of mercury species by clay minerals, Water Air Soil Pollut., 9 (1978) 23–31.
[9] G. Blanchard, M. Maunaye, G. Martin, Removal of heavy metals from waters by means of natural zeolites, Water Res., 18 (1984) 1501–1507.
[10] C.S. Kim, J.J. Rytuba, G.E. Brown, EXAFS study of mercury(II) sorption to Fe- and Al-(hydr)oxides. II. Effects of chloride and sulfate, J. Colloid Interface Sci., 270 (2004) 9–20.
[11] A.J. Tchinda, E. Ngameni, I.T. Kenfack, A. Walcarius, One-step preparation of thiol-functionalized porous clay heterostructures: application to Hg(II) binding and characterization of mass transport issues, Chem. Mater., 21 (2009) 4111–4121.
[12] S. Chiarle, M. Ratto, M. Rovatti, Mercury removal from water by ion exchange resins adsorption, Water Res., 34 (2000) 2971–2978.
[13] S.J.L. Billinge, E.J. McKymmy, M. Shatnawi, H.J. Kim, V. Petkov, D. Wermeille, T.J. Pinnavaia, Mercury binding sites in thiol-functionalized mesostructured silica, J. Am. Chem. Soc., 127 (2005) 8492–8498.
[14] B. Li, Y. Zhang, D. Ma, Z. Shi, S. Ma, Mercury nano-trap for effective and efficient removal of mercury(II) from aqueous solution, Nat. Commun., 5 (2014) 5537.
[15] J. Wang, X. Feng, C.W.N. Anderson, Y. Xing, L. Shang, Remediation of mercury contaminated sites – a review, J. Hazard. Mater., 221–222 (2012) 1–18.
[16] F. Fu, D.D. Dionysiou, H. Liu, The use of zero-valent iron for groundwater remediation and wastewater treatment: a review, J. Hazard. Mater., 267 (2014) 194–205.
[17] W. Yan, A.A. Herzing, C.J. Kiely, W.X. Zhang, Nanoscale zero-valent iron (nZVI): aspects of the core-shell structure and reactions with inorganic species in water, J. Contam. Hydrol., 118 (2010) 96–104.
[18] B.D. Gibson, C.J. Ptacek, M.B.J. Lindsay, D.W. Blowes, Examining mechanisms of groundwater Hg(II) treatment by reactive materials: an EXAFS study, Environ. Sci. Technol., 45 (2011) 10415–10421.
[19] C.G. Weisener, K.S. Sale, D.J. Smyth, D.W. Blowes, Field column study using zerovalent iron for mercury removal from contaminated groundwater, Environ. Sci. Technol., 39 (2005) 6306–6312.
[20] R. Hernandez, M. Zappi, C.-H. Kuo, Chloride effect on TNT degradation by zerovalent iron or zinc during water treatment, Environ. Sci. Technol., 38 (2004) 5157–5163.
[21] P.G. Tratnyek, M.M. Scherer, B. Deng, S. Hu, Effects of natural organic matter, anthropogenic surfactants, and model quinones on the reduction of contaminants by zero-valent iron, Water Res., 35 (2001) 4435–4443.
[22] E.J. Weber, Iron-mediated reductive transformations: investigation of reaction mechanism, Environ. Sci. Technol., 30 (1996) 716–719.
[23] A. Shimizu, M. Tokumura, K. Nakajima, Y. Kawase, Phenol removal using zero-valent iron powder in the presence of dissolved oxygen: roles of decomposition by the Fenton reaction and adsorption/precipitation, J. Hazard. Mater., 201–202 (2012) 60–67.
[24] S.M. Ponder, J.G. Darab, T.E. Mallouk, Remediation of Cr(VI) and Pb(II) aqueous solutions using supported, nanoscale zero-valent iron, Environ. Sci. Technol., 34 (2000) 2564–2569.
[25] C.B. Wang, W.X. Zhang, Synthesizing nanoscale iron particles for rapid and complete dechlorination of TCE and PCBs, Environ. Sci. Technol., 31 (1997) 2154–2156.
[26] A. Amirbahman, D.B. Kent, G.P. Curtis, P. Gary, M.C. Marvin-DiPasquale, Kinetics of homogeneous and surface-catalyzed mercury(II) reduction by iron(II), Environ. Sci. Technol., 47 (2013) 7204–7213.
[27] G. Kemmer, S. Keller, Nonlinear least-squares data fitting in Excel spreadsheets, Nat. Protoc., 5 (2010) 267–281.
[28] E. Tipping, S. Lofts, J.E. Sonke, Humic ion-binding model VII: a revised parameterisation of cation-binding by humic substances, Environ. Chem., 8 (2011) 225–235.
[29] H.A. Wiatrowski, S. Das, R. Kukkadapu, E.S. Ilton, T. Barkay, N. Yee, Reduction of Hg(II) to Hg(0) by magnetite, Environ. Sci. Technol., 43 (2009) 5307–5313.
[30] Y. Li, Q. Yue, B. Gao, Adsorption kinetics and desorption of Cu(II) and Zn(II) from aqueous solution onto humic acid, J. Hazard. Mater., 178 (2010) 455–461.
[31] H. Kerndorff, M. Schnitzer, Sorption of metals on humic acid, Geochim. Cosmochim. Acta, 44 (1980) 1701–1708.
[32] L.L Stookey, Ferrozine—a new spectrophotometric reagent for iron, Anal. Chem., 42 (1970) 779–781.
[33] L, Xie, C. Shang, Role of humic acid and ouinone model compounds in bromate reduction by zerovalent iron, Environ. Sci. Technol., 39 (2005) 1092–100.
[34] M.J. Avena, L.K. Koopal, Kinetics of humic acid adsorption at solid-water interfaces, Environ. Sci. Technol., 33 (1999) 2739–2744.
[35] T.S. Pasakarnis, M.I. Boyanov, M. Kemner, B. Mishra, E.J. O'Loughlin, G. Parkin, M.M. Scherer, Influence of chloride and Fe(II) content on the reduction of Hg(II) by magnetite, Environ. Sci. Technol., 47 (2013) 6987–6994.
[36] A.B.M. Giasuddin, S.R. Kanel, H. Choi, Adsorption of Humic Acid onto Nanoscale Zerovalent Iron and Its Effect on Arsenic Removal, Environ. Sci. Technol., 41 (2007) 2022–2027.
[37] J. Wo, M. Zhang, X. Cheng, X. Zhong, J. Xu, X. Xu, Hg^{2+} reduction and re-emission from simulated wet flue gas desulfurization liquors, J. Hazard. Mater., 172 (2009) 1106–1110.